

EVIDENCE FOR AN ADDITIONAL HEAT SOURCE IN THE WARM IONIZED MEDIUM OF GALAXIES

R. J. REYNOLDS, L. M. HAFFNER, AND S. L. TUFTE¹

Department of Astronomy, University of Wisconsin–Madison, 475 North Charter Street,
Madison, WI 53706; reynolds@astro.wisc.edu, haffner@astro.wisc.edu

Received 1999 July 9; accepted 1999 August 26; published 1999 September 29

ABSTRACT

Spatial variations of the [S II]/H α and [N II]/H α line intensity ratios observed in the gaseous halo of the Milky Way and other galaxies are inconsistent with pure photoionization models. They appear to require a supplemental heating mechanism that increases the electron temperature at low densities, n_e . This would imply that in addition to photoionization, which has a heating rate per unit volume proportional to n_e^2 , there is another source of heat with a rate per unit volume proportional to a lower power of n_e . One possible mechanism is the dissipation of interstellar plasma turbulence, which, according to Minter & Spangler, heats the ionized interstellar medium in the Milky Way at a rate of $\sim 1 \times 10^{-25} n_e$ ergs cm⁻³ s⁻¹. If such a source were present, it would dominate over photoionization heating in regions where $n_e \lesssim 0.1$ cm⁻³, producing the observed increases in the [S II]/H α and [N II]/H α intensity ratios at large distances from the galactic midplane as well as accounting for the constancy of [S II]/[N II], which is not explained by pure photoionization. Other supplemental heating sources, such as magnetic reconnection, cosmic rays, or photoelectric emission from small grains, could also account for these observations, provided they supply $\sim 10^{-5}$ ergs s⁻¹ per square centimeter of the Galactic disk to the warm ionized medium.

Subject headings: galaxies: ISM — Galaxy: halo — H II regions — ISM: general

1. INTRODUCTION

Although the warm ionized medium (WIM), also called the diffuse ionized gas, is a principal component of the interstellar medium in our Galaxy and others, the source of its ionization and heating is not understood (e.g., Reynolds 1995; Rand 1998). Observed line intensities, particularly the high values of [S II]/H α and [N II]/H α compared with those in traditional discrete H II regions surrounding O and early-B stars, suggest that photoionization by a dilute radiation field plays an important role (e.g., Domgörgen & Mathis 1994); both models and observations indicate that these emission lines originate primarily from warm ($\sim 10^4$ K) regions in which the hydrogen is nearly fully ionized (e.g., Sembach et al. 1999; Reynolds et al. 1998). It has been suggested by Miller & Cox (1993) and Dove & Shull (1994), for example, that Lyman continuum radiation originating from O stars penetrates the H I cloud layer and ionizes diffuse interstellar gas within the disk and lower halo. While O stars are the only known source with sufficient power to maintain the WIM, the high opacity of the interstellar H I has led others to propose the existence of more widely distributed sources of ionization (e.g., Slavin, Shull, & Begelman 1993; Mellott, McKay, & Ralston 1988; Sciamia 1990; Raymond 1992; Skibo & Ramaty 1993).

2. PROBLEMS WITH PURE PHOTOIONIZATION MODELS

Photoionization models incorporating a low-ionization parameter U (the ratio of photon density to gas density) have generally been successful in accounting for the elevated [S II]/H α and [N II]/H α and low [O III] $\lambda 5007$ /H α ratios observed in the WIM (e.g., Domgörgen & Mathis 1994; Greenawalt, Waltherbos, & Braun 1997; Martin 1997; Wang, Heckman, & Lehnert 1998). However, the models have failed to explain observed *variations* in some of the ratios. For example, Rand

(1998) observed that [S II]/H α and [N II]/H α increase with increasing distance $|z|$ from the midplane of NGC 891, having values of 0.2 and 0.35, respectively, near $z = 0$ and 0.6 and 1.0, respectively, near $|z| = 2000$ pc. To account for such large ratios at high $|z|$, Rand had to adopt a hard stellar spectrum (an upper initial mass function cutoff of $120 M_\odot$) plus additional hardening as the radiation propagated away from the midplane. However, a hard spectrum appears to be inconsistent with He I $\lambda 5876$ recombination line observations (Rand 1997, 1998, and references therein).

More significantly, the models fail to account for the fact that, while the variations in [S II]/H α and [N II]/H α are large, [S II]/[N II] remains nearly constant. A similar behavior for [S II], [N II], and H α has been observed in other galaxies (e.g., Golla, Dettmar, & Domgörgen 1996; Otte & Dettmar 1999) as well as in the Milky Way (Haffner, Reynolds, & Tufte 1999). Golla et al. (1996) and Rand (1998) have pointed out that the constant value of [S II]/[N II] cannot be reproduced by photoionization models because, in these models, variations in [S II]/H α and [N II]/H α are primarily the result of variations in the ionization parameter U ; these variations always produce larger changes in [S II]/H α than in [N II]/H α . This is due to the different ionization potentials of S and N, with the result that sulfur can be primarily S⁺ or primarily S⁺⁺, depending on the spectrum and strength of the radiation field, whereas nitrogen remains primarily N⁺ under nearly all WIM conditions (e.g., Howk & Savage 1999).

Another observation that pure photoionization models fail to reproduce is the rise in [O III]/H β with increasing $|z|$, or increasing [S II]/H α and [N II]/H α (Rand 1998; Greenawalt et al. 1997). In NGC 891, for example, the [O III]/H β intensity ratio more than doubles from 0.3 at $z = 0$ to about 0.75 at $|z| = 2000$ pc (Rand 1998). The models predict the opposite trend. Rand proposed an additional source of collisional ionization at high $|z|$ to account for the enhanced [O III] intensity,

¹ New address: Department of Physics, Lewis and Clark College, 0615 SW Palatine Hill Road, Portland, OR 97219; tufte@lclark.edu.

but he emphasized that this would still not explain the constancy of the [S II]/[N II] ratio.

We show that these line ratio variations could be explained by the existence of an additional source of heat in the diffuse ionized gas. In the following sections, we use recent emission-line data for the Milky Way, obtained with the Wisconsin H-Alpha Mapper (WHAM) spectrometer, to derive the required heating rates and place constraints on possible supplemental heating mechanisms.

3. LINE RATIO VARIATIONS DUE TO AN ADDITIONAL HEAT SOURCE

3.1. Evidence for Variations in Electron Temperature

Haffner et al. (1999) have shown that these emission-line observations can be readily explained if the large variations in [N II]/H α and [S II]/H α are due primarily to variations in the electron temperature T_e rather than to variations in the ionization parameter U . The constancy of [S II]/[N II] is then a consequence of the fact that the two lines have nearly the same excitation energy. Such temperature variations could also produce increases in [O III]/H β , perhaps eliminating the need for a secondary source of ionization. For the Milky Way, Haffner et al. (1999) found that an increase in T_e from 7000 K at $|z| = 500$ pc to approximately 10,000 K at 1500 pc would produce the observed factor of 3 increases in the [N II]/H α and [S II]/H α ratios while keeping [S II]/[N II] constant. Elevated temperatures have also been proposed by Bland-Hawthorn, Freeman, & Quinn (1997) to account for the anomalously high [N II]/H α in the diffuse gas at the outer edge of the disk of NGC 253. They concluded that the high ratio could not be explained by photoionization alone but required an additional heat source at large galactic radius that would “selectively heat the electrons without producing a higher ionization state of nitrogen.”

These emission-line data suggest that the regions with higher [S II]/H α and [N II]/H α ratios (i.e., higher temperatures) are regions not just at larger distances $|z|$ from the galactic midplane but, more generally, are regions with lower electron density. This is indicated by the strong anticorrelation between these line ratios and the H α intensity. This anticorrelation is apparent not only in the data that show increasing ratios with increasing $|z|$ but also in observations at constant $|z|$ (e.g., Rand 1998; Otte & Dettmar 1999; Domgörgen & Dettmar 1997; Golla et al. 1996; Ferguson, Wyse, & Gallagher 1996) and at large galactocentric radii (Bland-Hawthorn et al. 1997). A strong anticorrelation is also found in the observations of the Milky Way (Haffner 1999; Haffner et al. 1999), again, not only with increasing $|z|$ but also for lines of sight that sample just the relatively low $|z|$ gas in the local Orion arm. Since it is difficult to see how the integration length could affect the temperature, we conclude that variations that are correlated with H α intensity (i.e., emission measure) are actually variations correlated with density.

If the temperature in fact varies inversely with density in the diffuse ionized gas, then there must be an additional heat source that dominates over ionization heating at low densities. The heating rate per unit volume from photoionization is limited by recombination and is thus proportional to n_e^2 . The cooling rate per unit volume depends on electron-ion collisions and is also proportional to n_e^2 . Therefore, with only photoionization, T_e is nearly independent of n_e (although the density dependence of the ion ratios will have some effect on the equilibrium temperature). However, if an additional heating term were added

that was proportional to n_e , or did not depend on density at all, it would dominate at sufficiently low densities, increasing the equilibrium temperature and producing an inverse relationship between T_e and n_e (Reynolds & Cox 1992). This additional heating term would decouple the heating of the gas from its ionization, driving up the intensities of [S II] and [N II] relative to H α while not affecting the ionization states of S and N, i.e., allowing the [S II]/[N II] ratio to remain constant. Such heat sources in the WIM may include, for example, photoelectric heating by dust, the dissipation of interstellar turbulence, Coulomb collisions with cosmic rays, which are proportional to n_e (Draine 1978; Minter & Balser 1997; Skibo, Ramaty, & Purcell 1996), and magnetic field reconnection, which may be nearly independent of density (Gonçalves, Jatenco-Pereira, & Opher 1993).

3.2. Electron Temperature versus $|z|$ in the Perseus Arm

The heating rates due to both photoionization and the supplemental source can be estimated by fitting the predicted variation in [N II]/H α with temperature to the observed variation in this line ratio. This can be done for the Perseus spiral arm of the Milky Way, where the associated optical emission lines have been kinematically identified and observed to high Galactic latitude with the WHAM spectrometer (Haffner 1999; Haffner et al. 1999). As a result, these Perseus arm observations provide both line intensity ratios and electron densities as a function of distance from the Galactic midplane. Figure 1 presents the electron temperatures T_e versus $|z|$ derived from these [N II]/H α data and the relationship between T_e and [N II]/H α given by

$$\frac{I_{[\text{N II}]}}{I_{\text{H}\alpha}} = 1.63 \times 10^5 \left(\frac{\text{N}^+}{\text{N}}\right) \left(\frac{\text{H}^+}{\text{H}}\right)^{-1} \left(\frac{\text{N}}{\text{H}}\right) T_4^{0.426} e^{-2.18/T_4}, \quad (1)$$

where T_4 is T_e in units of 10^4 K, N/H is the gas-phase abundance of nitrogen, and N^+/N and H^+/H are the fraction of nitrogen and hydrogen, respectively, that is singly ionized. Since $\text{N}^+/\text{N} \approx \text{H}^+/\text{H}$ (e.g., Howk & Savage 1999; Haffner et al. 1999) and $\text{N}/\text{H} \approx 7.5 \times 10^{-5}$ (Meyer, Cardelli, & Sofia 1997), equation (1) can be rewritten simply as

$$\frac{I_{[\text{N II}]}}{I_{\text{H}\alpha}} = 12.2 T_4^{0.426} e^{-2.18/T_4}. \quad (2)$$

Equation (2) and the plot of [N II]/H α versus Galactic latitude presented in Figure 8 of Haffner et al. (1999) were then combined to produce the T_e versus $|z|$ relation for the Perseus arm in Figure 1. This result covers the Galactic latitude range $-34^\circ \geq b \geq -6^\circ$ averaged over the longitude interval $125^\circ \geq l \geq 152^\circ$. The distance to the Perseus arm is assumed to be 2.5 kpc (Reynolds et al. 1995 and references therein).

3.3. Electron Density versus $|z|$ in the Perseus Arm

The electron density n_e within the WIM at a distance $|z|$ from the midplane can be derived from the H α intensity, which is related to the emission measure (EM) through the relation $\text{EM} = 2.75 T_4^{0.9} I_{\text{H}\alpha}$ (from Martin 1988), where $\text{EM} (= n_e^2 ds)$ is in units of $\text{cm}^{-6} \text{pc}$ and $I_{\text{H}\alpha}$ is in rayleighs ($1 \text{ R} = 10^6/4\pi$ photons $\text{cm}^{-2} \text{s}^{-1} \text{sr}^{-1}$). Along the line of sight through the Perseus arm, the EM can be expressed as $n_e^2 fL$, where L is the path length through the arm, f is the fraction of L occupied by ionized

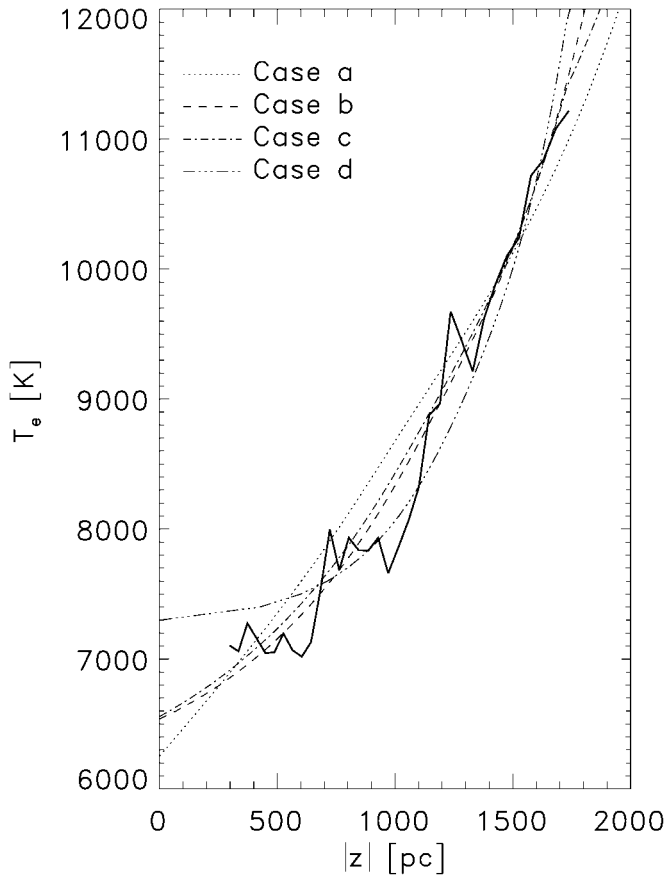


FIG. 1.—Electron temperatures T_e inferred from the $[\text{N II}]/\text{H}\alpha$ line intensity ratios plotted vs. the distance $|z|$ from the Galactic midplane in the Perseus spiral arm (*thick line*). Also plotted are the best fits to this T_e vs. $|z|$ relation for four cases in which the gas is heated by photoionization plus an additional nonionizing source (see text).

hydrogen, and n_e is the rms electron density within the ionized regions. Haffner et al. (1999) showed that for the same ranges of l and b represented in Figure 1, $I_{\text{H}\alpha}(|z|) \approx 5.7e^{-|z|/500}$ R. Therefore, if L is assumed to have a value of 1000 pc (see Fig. 1 in Becker & Fenkart 1970),

$$n_e(|z|) = 0.125T_4^{0.45}f^{-0.5}e^{-|z|/1000} \text{ cm}^{-3}. \quad (3)$$

We consider two situations: (1) a constant filling fraction $f = 0.2$ (Reynolds 1991) and (2) a filling fraction that increases with $|z|$ according to the relation given by Kulkarni & Heiles (1987), that is, $f(|z|) = 0.1e^{|z|/750}$ for $|z| < 1740$ pc. There is some evidence that f does in fact increase with distance from the midplane (Reynolds 1991); however, the results are sufficiently uncertain that both a constant and varying f are considered here.

3.4. Fits to the T_e versus $|z|$ Relation

We assume that the temperature is determined by a balance between the cooling rate per unit volume (Λn_e^2) in the diffuse ionized gas and two heating rates: the net heating by photoionization, given by $G_0 n_e^2$, plus an additional heating term, given either by $G_1 n_e$ or by just a constant G_2 . The heating-cooling balance can then be expressed as either $G_0 + G_1 n_e = \Lambda$ or $G_0 + G_2 n_e^2 = \Lambda$, representing, for example, supplemental heat-

TABLE 1
HEATING RATE COEFFICIENTS FOR THE PERSEUS ARM

Case	G_0 ($\times 10^{-24}$ ergs $\text{cm}^3 \text{s}^{-1}$)	G_1 ($\times 10^{-25}$ ergs s^{-1})	G_2 ($\times 10^{-27}$ ergs $\text{cm}^{-3} \text{s}^{-1}$)
a	0.3	1.6	...
b	0.95	...	7.6
c	0.9	0.65	...
d	1.35	...	1.5

ing by turbulent dissipation (G_1) or by magnetic field reconnection (G_2), respectively. Therefore, depending on the values of G_1 or G_2 relative to G_0 , significantly increased heating (relative to photoionization) can occur as the density decreases. This will result in higher equilibrium temperatures at lower densities.

We have adopted the cooling function Λ for low-density photoionized gas given in Osterbrock (1989). While this particular cooling function may not be exactly appropriate for the WIM, for $T_e > 7000$ K (the temperature range considered here), it is a very good approximation because, like the model H II region in Osterbrock, the WIM's cooling function is dominated by $[\text{O II}]$ and $[\text{N II}]$. An equilibrium temperature for each value of $|z|$ can be computed from equation (3) and one of the above heating-cooling balance equations. The values of G_0 and G_1 , or G_0 and G_2 , can then be adjusted to fit the T_e versus $|z|$ distribution in Figure 1. The best-fit values are listed in Table 1 for four cases: (a) supplemental heating $G_1 n_e$ and constant f ; (b) supplemental heating G_2 and constant f ; (c) supplemental heating $G_1 n_e$ and variable $f(|z|)$; and (d) supplemental heating G_2 and variable $f(|z|)$. The associated best-fit curves are also plotted in Figure 1 for comparison with the T_e versus $|z|$ inferred from the observed $[\text{N II}]/\text{H}\alpha$ ratios in the Perseus arm. Note that the derived values for G_1 and G_2 are proportional to $L^{-1/2}$ and L^{-1} , respectively, where L is the assumed path length through the Perseus arm. Also, Haffner et al. (1999) discussed the possible contamination of the $[\text{N II}]$ spectra by a weak atmospheric emission line. If this line is present with the intensity of their upper limit (0.1 R), then the best-fit values for G_1 and G_2 would be 20%–30% lower than those presented in Table 1, while G_0 would be less affected.

4. DISCUSSION

Figure 1 shows that all four cases give good fits to the inferred T_e versus $|z|$ distribution, within the uncertainty implied by the jaggedness of the distribution. Therefore, a supplemental heat source with a heating rate per unit volume proportional to n_e^1 or n_e^0 could account for the observed variations in the line intensity ratios. Moreover, these results place tight constraints on the required rates, implying a photoionization heating rate coefficient of $G_0 \approx 1 \times 10^{-24}$ ergs $\text{cm}^3 \text{s}^{-1}$ and a supplemental rate coefficient of either $G_1 \sim 1 \times 10^{-25}$ ergs s^{-1} or G_2 approximately a few times 10^{-27} ergs $\text{cm}^{-3} \text{s}^{-1}$. Thus, for $n_e > 1 \text{ cm}^{-3}$, the heating rate per unit volume is dominated by photoionization, while below $0.1\text{--}0.04 \text{ cm}^{-3}$, the supplemental heating dominates. This value for G_0 corresponds to a stellar ionizing spectrum with $T_{\text{eff}} \approx 30,000\text{--}35,000$ K (Osterbrock 1989), i.e., late O to early B, and is consistent with the observations of weak He I recombination line emission from the WIM (Tufté 1997; Reynolds & Tufté 1995; Heiles et al. 1996).

Values of G_1 near 1×10^{-25} ergs s^{-1} (Table 1) have in fact been predicted for the WIM in the Milky Way by models of photoelectric grain heating (Reynolds & Cox 1992; Draine

1978) and by models of the dissipation of interstellar turbulence (Minter & Spangler 1997). At electron temperatures above 8000 K, the net heating by grains decreases sharply because of cooling by electron-grain collisions (Draine 1978), and therefore this process is not likely to account for the 9000–11,000 K temperatures at high $|z|$, unless photoelectric heating in the WIM is dominated by large molecules (e.g., polycyclic aromatic hydrocarbons [PAHs]) (Lepp & Dalgarno 1988). Minter & Spangler (1997), on the other hand, have predicted an energy dissipation rate of approximately $1 \times 10^{-25} n_e$ ergs $\text{cm}^{-3} \text{s}^{-1}$ due to ion-neutral collisional dampening in the Milky Way's nearly fully ionized 10^4 K WIM. They concluded that the dissipation of turbulence probably plays a major role in heating the WIM and in contributing to the [S II] and [N II] emission (see also Minter & Balser 1997 and Tufte, Reynolds, & Haffner 1999). Another potential source is Coulomb collisions by cosmic rays, which, according to some interpretations of the Galactic γ -ray background, could deposit significant power into the interstellar gas (e.g., Skibo et al. 1996; Valinia & Marshall 1998).

A heating mechanism that is independent of density (curves *b* and *d* in Fig. 1) could also account for these temperature variations. One such mechanism is magnetic field reconnection (Raymond 1992; Birk, Lesch, & Neukirch 1998; Gonçalves et al. 1993). A field strength as high as $7 \mu\text{G}$ (Webber 1998; Heiles 1995) and a timescale of 10^8 yr for the amplification of the field by the Galactic dynamo (Raymond 1992 and references therein) would provide an average power of 6×10^{-28} ergs $\text{cm}^{-3} \text{s}^{-1}$, a rate that is a factor of 2.5–13 below the values for G_2 given in Table 1—but approximately the rate that is needed if reconnection occurred only within the more limited volume of the WIM.

5. SUMMARY AND CONCLUDING REMARKS

The anticorrelation between H α intensity and the line intensity ratios [N II]/H α and [S II]/H α , as well as the constancy of [N II]/[S II] in the diffuse ionized gas of the Milky Way and other galaxies, can be explained if the electron temperature T_e increases with decreasing density n_e . An inverse relationship between T_e and n_e would imply that, in addition to photoionization, which heats at a rate proportional to n_e^2 , there is an additional source that is proportional to a lower power of n_e .

In the Milky Way, the dissipation of interstellar turbulence, with a predicted rate of $\sim 1 \times 10^{-25} n_e$ ergs $\text{cm}^{-3} \text{s}^{-1}$ in the WIM (Minter & Spangler 1997), may be the source of this additional heating, raising the possibility that the observed increases in forbidden line intensities (relative to H α) in galactic halos is the final step in a turbulent energy cascade that begins with large-scale motions of the interstellar gas. However, other mechanisms, such as heating by PAHs, magnetic reconnection, or cosmic rays, are also possible provided that within the WIM, they have a rate coefficient of the magnitude listed in Table 1.

Measurements of higher T_e in regions with higher [N II]/H α and [S II]/H α would provide strong, independent support for the existence of such supplemental heating. These measurements could perhaps be made through accurate observations of the H α , [N II], and [S II] line widths (e.g., Reynolds 1985) or through observations of other emission lines such as [O II] $\lambda 3727$ and the extremely faint line [N II] $\lambda 5755$, which have higher excitation energies, and thus are more temperature sensitive, than [N II] $\lambda 6584$ and [S II] $\lambda 6716$ (see Ferguson et al. 1996). We hope to begin some of these investigations in the near future.

This work was supported by National Science Foundation grant AST 96-19424.

REFERENCES

- Becker, W., & Fenkart, R. 1970, in IAU Symp. 38, The Spiral Structure of Our Galaxy, ed. W. Beker & G. Contopoulos (Dordrecht: Reidel), 205
- Birk, G. T., Lesch, H., & Neukirch, T. 1998, MNRAS, 296, 165
- Bland-Hawthorn, J., Freeman, K. C., & Quinn, P. J. 1997, ApJ, 490, 143
- Domgörgen, H., & Dettmar, R.-J. 1997, A&A, 322, 391
- Domgörgen, H., & Mathis, J. S. 1994, ApJ, 428, 647
- Dove, J. B., & Shull, J. M. 1994, ApJ, 430, 222
- Draine, B. T. 1978, ApJS, 36, 595
- Ferguson, A. M. N., Wyse, R. F. G., & Gallagher, J. S. 1996, AJ, 112, 1267
- Golla, G., Dettmar, R.-J., & Domgörgen, H. 1996, A&A, 313, 439
- Gonçalves, D. R., Jatenco-Pereira, V., & Opher, R. 1993, ApJ, 414, 57
- Greenawalt, B., Walterbos, R. A. M., & Braun, R. 1997, ApJ, 483, 666
- Haffner, L. M. 1999, Ph.D. thesis, Univ. Wisconsin–Madison
- Haffner, L. M., Reynolds, R. J., & Tufte, S. L. 1999, ApJ, 523, 223
- Heiles, C. 1995, in ASP Conf. Ser. 80, The Physics of the Interstellar and Intergalactic Medium, ed. A. Ferrara, C. F. McKee, C. Heiles, & P. R. Shapiro (San Francisco: ASP), 507
- Heiles, C., Koo, B.-C., Levenson, N. A., & Reach, W. T. 1996, ApJ, 462, 326
- Howk, J. C., & Savage, B. D. 1999, ApJ, 517, 746
- Kulkarni, S., & Heiles, C. 1987, in Interstellar Processes, ed. D. J. Hollenbach & H. A. Thronson, Jr. (Dordrecht: Reidel), 87
- Lepp, S., & Dalgarno, A. 1988, ApJ, 335, 769
- Martin, C. L. 1997, ApJ, 491, 561
- Martin, P. G. 1988, ApJS, 66, 125
- Mellott, A. W., McKay, D. W., & Ralston, J. P. 1988, ApJ, 324, L43
- Meyer, D. M., Cardelli, J. A., & Sofia, U. J. 1997, ApJ, 490, L103
- Miller, W. W., III, & Cox, D. P. 1993, ApJ, 417, 579
- Minter, A. H., & Balser, D. S. 1997, ApJ, 484, L133
- Minter, A. H., & Spangler, S. R. 1997, ApJ, 485, 182
- Osterbrock, D. E. 1989, Astrophysics of Gaseous Nebulae and Active Galactic Nuclei (Mill Valley: University Science Books)
- Otte, B., & Dettmar, R.-J. 1999, A&A, 343, 705
- Rand, R. J. 1997, ApJ, 474, 129
- . 1998, ApJ, 501, 137
- Raymond, J. C. 1992, ApJ, 384, 502
- Reynolds, R. J. 1985, ApJ, 294, 256
- . 1991, ApJ, 372, L17
- . 1995, in ASP Conf. Ser. 80, The Physics of the Interstellar and Intergalactic Medium, ed. A. Ferrara, C. F. McKee, C. Heiles, & P. R. Shapiro (San Francisco: ASP), 388
- Reynolds, R. J., & Cox, D. P. 1992, ApJ, 400, L33
- Reynolds, R. J., Hausen, N. R., Tufte, S. L., & Haffner, L. M. 1998, ApJ, 494, L99
- Reynolds, R. J., & Tufte, S. L. 1995, ApJ, 439, L17
- Reynolds, R. J., Tufte, S. L., Kung, D. T., McCullough, P. M., & Heiles, C. 1995, ApJ, 448, 715
- Sciama, D. W. 1990, ApJ, 364, 549
- Sembach, K. R., Howk, J. C., Ryans, R. S. I., & Keenan, F. P. 1999, ApJ, in press
- Skibo, J. G., & Ramaty, R. 1993, A&AS, 97, 145
- Skibo, J. G., Ramaty, R., & Purcell, W. R. 1996, A&AS, 120, 403
- Slavin, J. D., Shull, J. M., & Begelman, M. C. 1993, ApJ, 407, 83
- Tufte, S. L. 1997, Ph.D. thesis, Univ. Wisconsin–Madison
- Tufte, S. L., Reynolds, R. J., & Haffner, L. M. 1999, in Interstellar Turbulence, ed. J. Franco & A. Carramiñana (Cambridge: Cambridge Univ. Press), 27
- Valinia, A., & Marshall, F. E. 1998, ApJ, 505, 134
- Wang, J., Heckman, T. M., & Lehnert, M. D. 1998, ApJ, 509, 93
- Webber, W. R. 1998, ApJ, 506, 329